Variational average atom in quantum plasmas (VAAQP)—first numerical results

2009 J. Phys. A: Math. Theor. 42 214059

(http://iopscience.iop.org/1751-8121/42/21/214059)

IOP PUBLISHING JOURNAL OF PHYSICS A: MATHEMATICAL AND THEORETICAL

J. Phys. A: Math. Theor. **42** (2009) 214059 (9pp) doi:10.1088/1751-8113/42/21/214059

Variational average atom in quantum plasmas (VAAQP)—first numerical results

R Piron[1], **T Blenski**[1] **and B Cichocki**[2]

[1] CEA, IRAMIS, Service des Photons Atomes et Molécules, F-91191 Gif-sur-Yvette, France
[2] Institute of Theoretical Physics, Warsaw University, Hoża 69, PL 00-681 Warsaw, Poland

E-mail: robin.piron@cea.fr

Received 14 October 2008, in final form 17 February 2009
Published 8 May 2009
Online at stacks.iop.org/JPhysA/42/214059

Abstract

A new code called VAAQP (variational average atom in quantum plasmas) is briefly described and its first results in the case of aluminium at solid density and temperatures between 0.05 and 12 eV are reported. The code is based on a new fully variational approach to plasmas at local equilibrium with both bound and free electrons treated quantum mechanically. This model which is derived from two first terms of the cluster expansion appears to be the quantum extension of the well-known atom-in-cell model based on the Thomas–Fermi theory (Thomas–Fermi average atom) that has been proposed in 1949 by Feynman, Metropolis and Teller. Similar to the case of Feynman *et al*'s model the VAAQP approach, due to its fully variational character, respects the virial theorem and uses a simple formula for the electronic pressure. Comparisons to results obtained using other approaches are also shown and discussed in the aluminium case. The results confirm the feasibility of the quantum variational model in the warm dense matter regime. Effects of the variational treatment can lead in this regime to significant differences with respect to existing non-variational models.

PACS numbers: 52.25.Kn, 52.25.Jm, 52.27.Gr

1. Introduction

We present here a code called VAAQP which is a numerical application of a new fully variational plasma model with all quantum electrons. Models of plasmas at local thermodynamic equilibrium with quantum bound and free electrons are necessary in order to calculate the photo-absorption cross sections and the equation of state in the modelling of inertial fusion devices, in astrophysics, in laboratory plasma studies and in warm dense matter experiments. Up to now the existing average-atom models in which all electrons

are treated as quantum [1–3] have not been fully variational in the sense that they were not respecting the virial theorem. Recently, a fully variational model with all quantum electrons respecting the virial theorem has been proposed [4, 5]. This variational model is in our opinion a first relatively simple and coherent model of plasma matter with quantum electrons. Atomic structure calculations and electronic pressure obtained from this model are in principle thermodynamically coherent. The structure elements can be used further to calculate plasma radiative and transport properties consistent with the equation of state.

One may expect our model to work well in the case of strongly coupled plasmas in which the ion–ion correlation function has roughly the form of a cavity (as it will be explicitly stated in section 2). We focus our attention here on the electronic structure. This model may be supplemented by different approximations to ion free energy and pressure contributions.

Among the most interesting applications of plasma models are cases corresponding to the warm dense matter (WDM) regime. Special attention is thus paid to matter at high density (i.e. solid density) and relatively low temperature (around a few eV or below). However this regime is also the most difficult to account for in the VAAQP code. The main reason for this difficulty is the presence of the long-range Friedel oscillations. For this reason in this preliminary study we focus our attention on a WDM case for aluminium.

This paper is organized as follows. Section 2 contains a short review of the model. Section 3 is devoted to a brief description of the VAAQP code. Some results obtained with the code for aluminium (Al) in the WDM regime are presented in section. 4. Differences between models requiring the neutrality of the Wigner-Seitz (WS) sphere (like in the INFERNO model [1, 3]) and the variational model are discussed in this section. We recall that the WS sphere radius R_{WS} is simply related to the ion density n_i by the formula: $R_{\mathrm{WS}} = (3/(4\pi n_i))^{1/3}$. Comparisons with experiments and state-of-the-art simulations are presented in section 5.

2. Variational theory of the average atom in jellium

The VAAQP code uses a new model [4, 5] of plasma at thermodynamical equilibrium with bound and continuum electrons treated within the same formalism. In this model, the plasma equilibrium is determined by three parameters: atomic number Z, temperature T and ion density n_i. All other quantities, including mean ionization Z^*, can be determined from variational equations using for instance the density functional theory (DFT). As shown in [4, 5] in the Thomas–Fermi (TF) approximation to the electron density the present model leads naturally to the TF ion-in-cell approach proposed in 1949 by Feynman *et al* [6].

The starting point of the present model is the cluster expansion [7–9] of the free energy per unit volume from which the two first orders are retained:

$$f(n_i, Z, T) = f_0 + \langle f \rangle_1 + \cdots, \tag{1}$$

where f_0 is the free energy per unit volume of a uniform electron gas with an unknown density n_0,

$$n_0 = n_i Z^* \tag{2}$$

In the zeroth order, electron charge density is neutralized by a uniform ion background. $\langle f \rangle_1$ is the average contribution to the free energy density of one ion immersed in that jellium. In the first order the system is no more homogeneous. The cluster expansion in the first order leads to

$$\langle f \rangle_1 = n_i \int \mathrm{d}^3 r \left\{ f_1^{\text{ion+jellium}}(X; n_i, Z, T; \vec{r}) - f_0(n_0, T) \right\}. \tag{3}$$

The subtraction of the zeroth-order term assures the convergence of the above integral. In what follows all structure variables, including n_0, will be denoted by X.

The free energies per ion are thus defined as follows:

$$F(X; n_i, Z, T) = F_0 + \Delta F_1 = \frac{f_0(n_0, T)}{n_i} + \frac{\langle f \rangle_1}{n_i}. \tag{4}$$

All structure variables X are determined from the minimization of the free energy $F(X; n_i, Z, T)$ with additional conditions:

- In the first order, we assume that the non-central ions are absent inside a cavity with a radius R

$$n_0 \theta(r - R). \tag{5}$$

- The neutrality of all charges, including the cavity, leads to the equation

$$Z + \int \mathrm{d}^3 r \{n(\vec{r}) - n_0 \theta(r - R)\} = 0. \tag{6}$$

- The total electron number per unit volume has the following cluster expansion:

$$Z n_i = n_0 + n_i \int \mathrm{d}^3 r \{n(\vec{r}) - n_0\} + \cdots. \tag{7}$$

Substituting equation (7) into equation (6) leads to the identity: $R = R_{\mathrm{WS}}$

The minimization leads to self-consistent-field (SCF) equations similar to those obtained in [1–3] plus a new one which allows us to determine n_0 or Z^*:

$$\int \mathrm{d}^3 r \{V_{\mathrm{el}}(\vec{r}) \theta(r - R)\} = 0, \tag{8}$$

where $V_{\mathrm{el}}(r)$ is the electrostatic part of the SCF potential [4, 5].

It is interesting to note that equation (8) means that in the model, the electronic SCF potential does not interact with the non-central ions charge distribution. There is a possibility to extend this model to other non-central ions charge distributions. This subject will not be considered in the present paper.

The main difference between INFERNO-type models [1, 3] and the present one is the determination of the mean ionization Z^*. In the INFERNO type models, the mean ionization is obtained from the neutrality of the WS sphere whereas in the present one it is obtained from the variational principle (8). In the present model, the WS sphere is in general non-neutral.

3. The VAAQP code

The VAAQP code finds the solution to the variational equations described above (see equations (1)–(8)). First, a family of solutions to the SCF equations in the four-parameter space (Z, T, n_i, Z^*) is calculated. Among them is found such that fulfils equation (8) (see figure 1). The code has three options to calculate the electron density: semiclassical (TF), quantum-non-relativistic (Schrödinger) or quantum-relativistic (Dirac) formalism.

In the case of calculations using quantum density models, continuum state contributions to observables are integrated over energy using a resonance-catching adaptative-mesh-refinement method. The SCF solutions in the four-parameter space (Z, T, n_i, Z^*) are obtained by iteration using the method described in [10]. The electron density and total potential are calculated using finite difference numerical methods inside the region extending from the radius equal to zero up to an asymptotic radius. At this radius the electron density is matched to its asymptotic form which is calculated using the linear response theory of a homogeneous dense plasma [11, 12]. Solutions are considered valid if they are insensitive to the choice of the matching

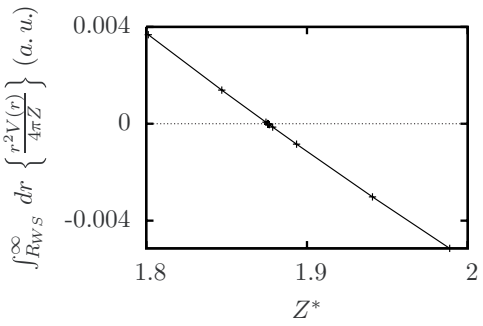

Figure 1. Left-hand term of equation (8) versus Z^*. Example of solution in the case of Al plasma at 5 eV temperature and 2.7 g cm^{-3} matter density. Each point on the figure corresponds to a SCF solution in the four-parameter space (Z, T, n_i, Z^*).

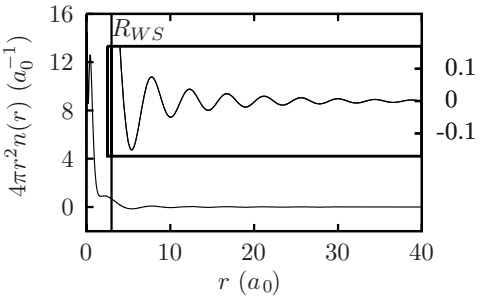

Figure 2. Plot of the electron density versus radius for Al at 0.25 eV temperature and 2.7 g cm^{-3} matter density with an enlarged view of the Friedel oscillations.

radius and are not mesh dependent. The matching radius depends mostly on the range of the Friedel oscillations and becomes larger as temperature is lower (see figure 2).

Instead of looking for solution to equation (8), the code has other options allowing one to fulfil other conditions as for instance the neutrality of the WS sphere.

4. Model comparison in the case of the warm dense aluminium

The code has been applied in the case of Al at typical condition of WDM, i.e. solid density (2.7 g cm^{-3}) and temperatures between 0.05 and 12 eV. In this regime, Friedel oscillations decay on a scale much larger than the WS radius (decay length $\left(2.b_0^F\right)^{-1} = 55.2\,a_0$ at 0.05 eV temperature, WS radius $R_{\mathrm{WS}} = 2.99\,a_0$; $b_0^F = \mu^{1/2}(-1 + \sqrt{1 + (\pi T/\mu)^2})^{1/2}$ is the imaginary part of the zeroth-order pole of the Fermi–Dirac function). In such cases, the region of numerical calculations should extend over several tens of R_{WS}. It is important to recall that the present approach is based on the assumption that the SCF potential decays exponentially due to screening and decay of the Friedel oscillations which is only valid at finite temperatures [11, 12].

The exchange-correlation term is taken in the local density approximation (LDA). For this exploratory study, in order to have direct comparisons with the Thomas–Fermi–Dirac (TFD) model, Dirac exchange term [13, 14] was used. Iyetomi and Ichimaru finite-temperature exchange-correlation term [15] has also been tested. In the temperature regime of interest in

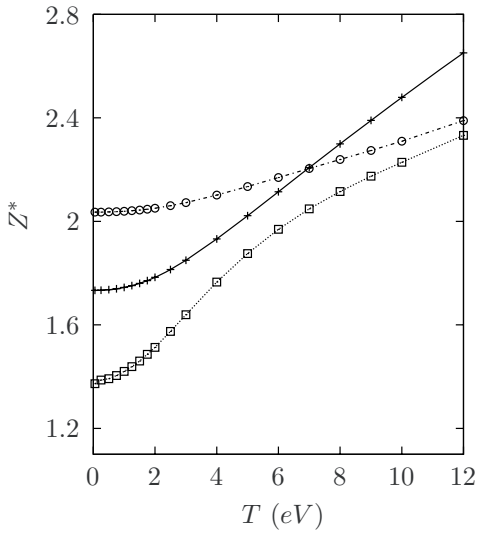

Figure 3. Mean ionization Z^* as defined in equation (2) versus temperature in the case of Al at 2.7 g cm^{-3} matter density. Solid line corresponds to the variational model with TF density. Plus symbols denote the neutral WS sphere model with TF density. Squares correspond to the variational model with non-relativistic quantum density. Circles denote the neutral WS sphere model with non-relativistic quantum density.

this study, the differences between results obtained using these two approximations appeared to be relatively small.

Figure 3 displays the behaviour of the mean ionization Z^* that was defined in equation (2). This definition is the only one justified in the framework of the TF and quantum cases [5] and can be also applied to any model as it corresponds to the asymptotic value n_0 of the electron density, which is related to the chemical potential. Other definitions related to the total electron density are sometimes used. One of those is the value of the electron density at the WS radius. This definition is motivated by the fact that it is identical to the one related to n_0 in the TF case. Another possible definition could be the difference between the atomic number Z and the sum of the bound levels occupation numbers. However, definitions of the number of bound (or free) electrons per atom relying on the summation of the occupations of bound (or localized free) states encounter well-known difficulties due to the fact that they are not related to any well-defined quantum operator. Definitions other than equation (2) will not be considered in this paper.

Results of four approaches are presented in figure 3. The first one is the result of the variational model with calculated non-relativistic quantum density. The second one is the result of the model with electron density calculated using the non-relativistic quantum density but in which equation (8) is replaced by the condition of the neutrality of the WS sphere (we call this approach NWS after 'neutral WS sphere'):

$$Z = \int_{|\vec{r}| \leqslant R_{\mathrm{WS}}} \mathrm{d}^3 r n(\vec{r}) \tag{9}$$

The condition based on equation (9) is used in the INFERNO model. However, calculations reported here with equation (9) do not correspond exactly to the original INFERNO model as in our case the potential outside the WS sphere is not equal to zero which is the case in that model. Two calculations using the TF formalism are also reported, one with equation (8),

another with equation (9). According to [4, 5], in the TF case, these two approaches are strictly equivalent which is confirmed by figures 3 and 4.

As it can be observed in figure 3, results from quantum calculations with equation (8) can differ significantly from those obtained by using equation (9). Differences are especially pronounced at low temperature and tend to vanish as the temperature increases. It appears also that in the case of Al at solid density and at temperature below 2.5 eV, the atomic structure is different in the two quantum models. The 3s shell is found to exist within the variational model whereas it is absent when using the NWS model. These differences are mainly related to the quantum behaviour of the density outside the WS sphere, namely to the Friedel oscillations which are present in this regime.

Electronic pressure is calculated from the formula

$$P = -f_0 + n_0(\mu + V_{xc}(n_0) + V_{\mathrm{el}}(R_{\mathrm{WS}})). \tag{10}$$

$f_0 = f_0^0 + f_0^{xc}$ is the free energy per unit volume of a uniform electron gas including exchange correlation. f_0^0 is the ideal gas free energy for the grand-canonical ensemble, namely in atomic units

$$f_0^0 = -\frac{2}{3}\frac{\sqrt{2}}{\pi^2}T^{5/2}I_{3/2}\left(\frac{\mu}{T}\right) + n_0\mu. \tag{11}$$

In the present study f_0^{xc} was set to ϵ_{xc} from [14]. V_{xc} is the exchange-correlation part of the SCF potential [4, 5]

$$V_{xc}(n) = \frac{\partial f_0^{xc}(n)}{\partial n} = -\left(\frac{3n}{\pi}\right)^{1/3}. \tag{12}$$

Equation (10) is obtained from the variational theory and applies only to the case where equation (8) is fulfilled. The quantum NWS model is not variational and the use of the above pressure formula is only given for comparison purposes. In the case of models that are not fully variational the electronic pressure is often calculated by numerical differentiation of the free energy with respect to the ion density.

As can be seen in figure 4, relative differences in calculated pressures from the two quantum models can be about 40% in the low temperature region and decrease as temperature increases. Pressures obtained using the quantum NWS model at low temperatures seem to be relatively close to those obtained from the TFD model.

Figures 3 and 4 both display curves that are continuous with respect to temperature. In the case of the quantum variational model, it is worth stressing that continuity is preserved despite the fact that the 3s shell is disappearing between 2 and 2.5 eV. This is due to a careful treatment of continuum resonance in the VAAQP code.

5. Comparison with experiments and simulations

VAAQP provides only electronic contribution to the pressure. In order to compare our results to experiments and simulations in the regime of interest in this paper, we need to add an ion contribution to the pressure. We have chosen to use the simple formula given in [16, 17] which is based on Hansen's one-component plasma (OCP) simulations. Here, this contribution is of the order of about 20% or less. Following Mazevet and Zerah, we have calculated several mass density–temperature points corresponding to the SESAME 3700 principal Hugoniot curve (see [18] and references therein). In figure 5 are displayed results from those variational quantum calculations as well as available experimental data from [19–42]. Mazevet and Zerah simulation results are also shown for comparison.

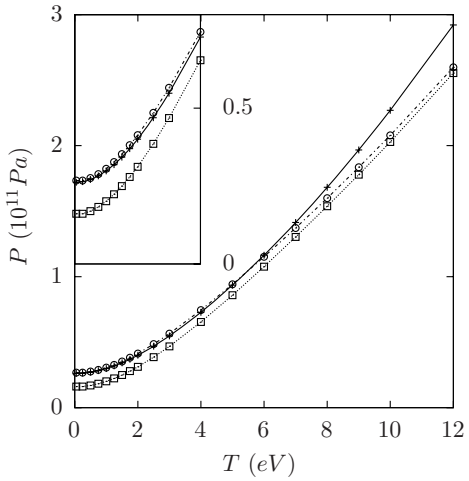

Figure 4. Electronic pressure P versus temperature in the case of Al at 2.7 g cm^{-3} matter density. Solid line corresponds to the variational model with TF density. Plus symbols denote the neutral WS sphere model with TF density. Squares correspond to the variational model with non-relativistic quantum density. Circles denote the neutral WS sphere model with non-relativistic quantum density.

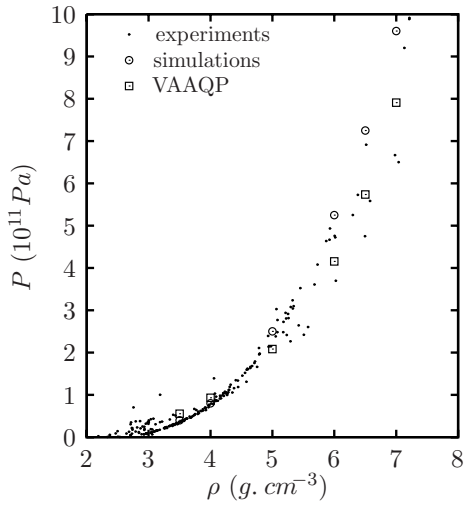

Figure 5. Comparison along the principal Hugoniot of Al between VAAQP variational quantum calculations, *ab initio* simulations from [18] and experiments from [19–42]. Total pressure P versus mass density ρ is presented.

This first comparison indicates that the pressure results compare rather well with experiments and state-of-the-art *ab initio* simulations in this region which is especially difficult from the numerical point of view in our case.

6. Conclusion

In this paper, a fully variational model of the average atom in quantum plasmas is applied for the first time in a numerical code called VAAQP. It is shown on some chosen examples that

the code is able to calculate variational self-consistent equilibrium at high matter density and relatively low temperatures. In this regime, Friedel oscillations of the electron density and SCF potential present a real challenge from the numerical point of view.

Effects of the variational treatment are studied by comparison to results from a model requiring the neutrality of the WS sphere. The variational model can lead to electronic pressures, mean ionizations and atomic structures that differ significantly from those obtained using existing models especially in the low temperature region.

Comparisons with experiments and *ab initio* simulations are also shown. Let us recall however that the main objectives of this work is to open the way to atomic physics and radiative properties calculations which could be coherent with the variational equation of state and the virial theorem. Such calculations can be based on methods similar to that used in the VAAQP code.

The work on the present model is in progress. Among objectives is the application of the method presented in this paper to the superconfigurations as indicated in [5].

Acknowledgments

The authors would like to thank C Bowen and J C Pain for their careful rereading of the manuscript. This work has been supported by the European Communities under the contract of association between EURATOM and CEA within the framework of the European Fusion Program. The views and opinions expressed herein do not necessarily reflect those of the European Commission.

References

[1] Liberman D A 1979 Self-consistent field model for condensed matter *Phys. Rev.* B **20** 4981–89
[2] Perrot F *CEA Internal Report*
[3] Wilson B, Sonnad V, Sterne P and Isaacs W 2006 Purgatorio—a new implementation of the Inferno algorithm *J. Quantum Spectrosc. Radiat. Transfer* **99** 658–79
[4] Blenski T and Cichocki B 2007 Variational approach to the average-atom-in-jellium and superconfigurations-in-jellium models with all electrons treated quantum-mechanically *High Energy Density Phys.* **3** 34–47
[5] Blenski T and Cichocki B 2007 Variational theory of average-atom and superconfigurations in quantum plasmas *Phys. Rev.* E **75** 056402
[6] Feynman R P, Metropolis N and Teller E 1949 Equation of state of elements based on the generalized Fermi–Thomas theory *Phys. Rev.* **75** 1561–73
[7] Felderhof B U, Ford G W and Cohen E G D 1982 Cluster expansion for the dielectric constant of a polarizable suspension *J. Stat. Phys.* **28** 135–64
[8] Blenski T and Cichocki B 1992 Linear response of partially ionized, dense plasmas *Laser Part. Beams* **10** 299–309
[9] Felderhof B U, Blenski T and Cichocki B 1995 Dielectric function of an electron–ion plasma in the optical and x-ray regime *Physica* A **217** 161–74
[10] Jena P and Singwi K S 1978 Electronic structure of hydrogen in simple metals *Phys. Rev.* B **17** 3518–24
[11] Khanna F C and Glyde H R 1976 Dynamic susceptibility of fermi liquids at finite temperature *Can. J. Phys.* **54** 648–54
[12] Gouedard C and Deutsch C 1978 Dense electron-gas response at any degeneracy *J. Math. Phys.* **19** 32–8
[13] Dirac P A M 1930 Note on exchange phenomena in the Thomas atom *Proc. Camb. Phil. Soc.* **26**
[14] Kohn W *et al* 1965 Self-consistent equations including exchange and correlation effects *Phys. Rev.* **140** A1133–A1138
[15] Iyetomi H and Ichimaru S 1986 Free energies of electron-screened ion plasmas in the hypernetted-chain approximation *Phys. Rev.* A **34** 433–9
[16] Hansen J P 1973 Statistical mechanics of dense ionized matter: I. Equilibrium properties of the classical one-component plasma *Phys. Rev.* A **8** 3096–109

[17] Nikiforov A F, Novikov V G and Uvarov V B 1987 Application of the quasiclassical approximation to a modified Hartree–Fock–Slater model *Teplofiz. Vys. Temp.* **25** 12–21
[18] Mazevet S and Zérah G 2008 Ab initio simulations of the K-edge shift along the aluminum Hugoniot *Phys. Rev. Lett.* **101** 155001
[19] Al'tshuler L V, Kormer S B, Bakanova A A and Trunin R F 1960 Equations of state for aluminum, copper and lead in the high pressure region *Zh. Eksp. Teor. Fiz.* **38** 790–8
[20] Al'tshuler L V, Kormer S B, Brazhnik M I, Vladimirov L A, Speranskaya M P and Funtikov A I 1960 The isentropic compressibility of aluminum, copper, lead at high pressures *Zh. Eksp. Teor. Fiz.* **38** 1061–73
[21] Al'tshuler L V and Petrunin A P 1961 Rentgenographic investigation of compressibility of light substances under obstacle impact of shock waves *Zh. Tekh. Fiz.* **31** 717–25
[22] Kormer S B and Funtikov A I 1962 Dynamical compression of porous metals and the equation of state with variable specific heat at high temperatures *Zh. Eksp. Teor. Fiz.* **42** 686–701
[23] Skidmore I C and Morris E 1962 Experimental equation-of-state data for uranium and its interpretation in the critical region *Thermodynamics of Nuclear Materials* (Vienna: IAEA) pp 173–216
[24] Isbell W H, Shipman F H and Jones A H 1968 Hugoniot equation of state measurements for eleven materials to five megabars *Mat. Sci. Lab.* vol MSL-68-13 (General Motors Corp.)
[25] McQueen R G, Marsh S P, Taylor J W, Fritz J N and Carter W J 1970 The equation of state of solids from shock wave studies *High Velocity Impact Phenomena* (New York: Academic) pp 293–417, 515
[26] Al'tshuler L V and Chekin B S 1974 Metrology of high pulsed pressures pp 5–22 Proc. 1st All-Union Pulsed Pressures Symp. vol 1
[27] Bakanova A A, Dudoladov I P and Sutulov Yu N 1974 Shock compressibility of porous tungsten, molybdenum, copper, and aluminum in low pressure range *Zh. Prikl. Mekh. Tekh. Fiz.* **2** 117–22
[28] Al'tshuler L V, Kalitkin N N, Kuz'mina L V and Chekin B S 1977 Shock adiabats for ultrahigh pressures *Zh. Eksp. Teor. Fiz.* **72** 317–25
[29] van Thiel M (ed) 1977 Compendium of shock wave data *Lawrence Livermore Laboratory Report UCRL-50108* 85–90
[30] Marsh S P (ed) 1980 *LASL Shock Hugoniot Data* (Berkeley, CA: University of California Press)
[31] Al'tshuler L V, Bakanova A A, Dudoladov I P, Dynin E A, Trunin R F and Chekin B S 1981 Shock adiabats for metals. new data, statistical analysis and general regularities *Zh. Prikl. Mekh. Tekh. Fiz.* **2** 3–34
[32] Volkov L P, Voloshin N P, Vladimirov A S, Nogin V N and Simonenko V A 1981 Shock compressibility of aluminum at pressure 10 mbar *Pis'ma Zh. Eksp. Teor. Fiz.* **31** 623–7
[33] Mitchell A C and Nellis W J 1981 Shock compression of aluminum, copper and tantalum *J. Appl. Phys.* **52** 3363–74
[34] Simonenko V A, Voloshin N P, Vladimirov A S, Nagibin A P, Nogin V P, Popov V A, Sal'nikov V A and Shoidin Yu A 1985 Absolute measurements of shock compressibility of aluminum at pressures $p \geqslant 1$ tPa *Zh. Eksp. Teor. Fiz.* **88** 1452–9
[35] Trunin R F 1986 Compressibility of various substances at high shock pressures *Izv. Akad. Nauk SSSR Fiz. Zemli* **2** 26–43
[36] Glushak B L, Zharkov A P, Zhernokletov M V, Ternovoi V Ya, Filimonov A S and Fortov V E 1989 Experimental investigation of the thermodynamics of dense plasmas formed from metals at high energy concentrations *Zh. Eksp. Teor. Fiz.* **96** 1301–18
[37] Trunin R F, Panov N V and Medvedev A B 1995 Compressibilities of iron, aluminum, molybdenum, titanum and tantalum at shock pressures of 1-2.5 tpa *Pis'ma Zh. Eksp. Teor. Fiz.* **62** 572–5
[38] Trunin R F, Podurets M A, Simakov G V, Popov L V and Sevast'yanov A G 1995 New data on aluminum, plexiglas and quartz compression obtained in strong shock wave of underground nuclear explosion *Zh. Eksp. Teor. Fiz.* **108** 851–61
[39] Trunin R F, Panov N V and Medvedev A B 1995 Shock compressibilities of iron, aluminum and tantalum at terapascal pressures *Chem. Phys.* **14** 97–9
[40] Trunin R F, Gudarenko L F, Zhernokletov M V and Simakov G V 2001 *Experimental Data on Shock Compressibility and Adiabatic Expansion of Condensed Substances* (Sarov, Russia: RFNC)
[41] Knudson M D, Lemke R W, Hayes D B, Hall C A, Deeney C and Asay J R 2003 Near-absolute Hugoniot measurements in aluminum to 500 GPa using a magnetically accelerated flyer plate technique *J. Appl. Phys.* **94** 4420–31
[42] Podurets M A, Simakov G V and Trunin R F 1990 Transition of stishovite to a denser phase *Izv. Akad. Nauk SSSR. Fiz. Zemli* **4** 30–7